



1                   **Interaction between Dicarboxylic Acid and Sulfuric Acid-Base Clusters**

2                                   **Enhances New Particle Formation**

3           Yun Lin,<sup>1</sup> Yuemeng Ji,<sup>1,2,\*</sup> Yixin Li,<sup>1</sup> Jeremiah Secrest,<sup>1</sup> Wen Xu,<sup>3</sup> Fei Xu,<sup>4</sup> Yuan Wang,<sup>5</sup>

4                                   Taicheng An,<sup>2</sup> and Renyi Zhang<sup>1,\*</sup>

5                   <sup>1</sup>Department of Atmospheric Sciences and Department of Chemistry, Texas

6                                   A&M University, College Station, TX 77843, USA

7           <sup>2</sup>Institute of Environmental Health and Pollution Control, Guangdong University of Technology,

8                                   Guangzhou 510006, China

9                                   <sup>3</sup>Aerodyne Research Inc, Billerica, MA 01821, USA

10           <sup>4</sup>School of Environmental Science and Engineering, Shandong University, Jinan 250100, China

11           <sup>5</sup>Division of Geological and Planetary Sciences, California Institute of Technology, Pasadena,

12                                   CA, 91125, USA

13           \* Corresponding authors: Renyi Zhang, [renyi-zhang@tamu.edu](mailto:renyi-zhang@tamu.edu); Yuemeng Ji, [jiym99@163.com](mailto:jiym99@163.com)



14 **ABSTRACT.** Dicarboxylic acids are believed to stabilize pre-nucleation clusters and facilitate  
15 new particle formation in the atmosphere, but the detailed mechanism leading to the formation of  
16 multi-component critical nucleus involving organic acids, sulfuric acid (SA), base species, and  
17 water remains unclear. In this study, theoretical calculations are performed to elucidate the  
18 interactions between succinic acid (SUA) and clusters consisting of SA-ammonia  
19 (AM)/dimethylamine (DMA) in the presence of hydration of up to six water molecules. Formation  
20 of the hydrated SUA·SA·base clusters by adding one SUA molecule to the SA·base hydrates is  
21 energetically favorable. The addition of SUA to the SA·base hydrates either triggers proton  
22 transfer from SA to the base molecule, resulting in formation of new covalent bonds, or strengthens  
23 the pre-existing covalent bonds. The presence of SUA promotes hydration of the SA·AM and  
24 SA·AM·DMA clusters but dehydration of the SA·DMA clusters. At equilibrium, the uptake of  
25 SUA competes with the uptake of the second SA molecule to stabilize the SA·base clusters at  
26 atmospherically relevant concentrations. The clusters containing both the base and organic acid  
27 are capable of further binding with acid molecules to promote their subsequent growth. Our results  
28 indicate that the multi-component nucleation involving organic acids, sulfuric acid, and base  
29 species promotes new particle formation in the atmosphere, particularly under polluted conditions.

30

31



## 32 1. INTRODUCTION

33 Atmospheric aerosols are important to several issues, including climate, visibility and  
34 human health (IPCC, 2013; Zhang et al., 2015). In particular, aerosols influence the Earth energy  
35 budget directly by absorbing/scattering incoming solar radiation and indirectly by acting as cloud  
36 condensation nuclei (CCN)/ice nuclei (IN), which impact the lifetime, coverage, precipitation  
37 efficiency, and albedo of clouds (Andreae et al., 2004; Fan et al., 2007; Li et al., 2008). Currently,  
38 the indirect radiative forcing of aerosols represents the largest uncertainty in climate predictions  
39 (IPCC, 2013). New particle formation (NPF) has been observed under diverse environmental  
40 conditions (Kulmala and Kerminen, 2008; Zhang et al., 2012; Guo et al., 2014; Bianchi et al., 2016;  
41 Wang et al., 2016) and contributes up to half of the CCN population in the troposphere (Merikanto  
42 et al., 2009; Yue et al., 2011). NPF involves two distinct steps, i.e., nucleation to form a critical  
43 nucleus and subsequent growth of newly formed nanoparticles to a larger size ( $> 3$  nm). Currently,  
44 the identities and the roles of chemical species involved in NPF are not fully understood at the  
45 molecular level, hindering the development of physically-based parameterization to include NPF  
46 in atmospheric models (Zhang et al. 2010; Cai and Jiang, 2017). Sulfuric acid (SA) is believed to  
47 be the most common atmospheric nucleation species, and ammonia (AM)/amines further stabilize  
48 the hydrated sulfuric acid clusters and enhance the nucleation (Kuang et al, 2010; Yue et al., 2010;  
49 Erupe et al., 2011; Yu et al., 2012; Qiu et al., 2013; Wang et al., 2018; Yao et al., 2018). However,  
50 neither the sulfuric acid-water binary nucleation nor ammonia/amine-containing ternary  
51 nucleation sufficiently explains the measured NPF rates in the lower troposphere (Xu et al., 2010a;  
52 Zhang et al. 2012), suggesting the role of other chemical species, such as organic acids, in NPF  
53 (Zhang et al., 2004; McGraw and Zhang, 2008).



54           The role of organic species in assisting aerosol nucleation and growth has been  
55 demonstrated by both experimental and theoretical studies (Zhang et al., 2009; Zhao et al., 2009;  
56 Wang et al., 2010; Xu et al., 2010b; Xu et al., 2012; Elm et al., 2014; Weber et al., 2014; Xu et al.,  
57 2014; Zhu et al., 2014; Tröstl et al., 2016). However, the interactions between organic acids and  
58 the other nucleation precursors are still elusive, due to the large variability in the physicochemical  
59 nature of organic acids, e.g., the wide range of volatility and functionality (Zhang et al., 2012;  
60 Riccobono et al., 2014). In addition, most of the previous theoretical studies focus on the  
61 enhancement effects of organic acids on the SA-H<sub>2</sub>O binary nucleation or the role of organic acids  
62 in clustering basic species such as ammonia or amines with hydration (Zhao et al., 2009; Xu et al.,  
63 2010; Xu et al. 2013; Elm et al., 2014; Weber et al., 2014; Zhu et al., 2014). Several recent studies  
64 have been conducted on the underlying mechanisms of organic acids in large pre-nucleation  
65 clusters (e.g. ammonia/amine-containing ternary nucleation) (Xu et al., 2010; Xu et al., 2012; Elm  
66 et al., 2016; Zhang et al., 2017), but most of these studies treated the clusters without the  
67 consideration of hydration. Because of the ubiquitous presence of water (W) in the atmosphere  
68 and its much higher abundance than other nucleation precursors, the hydration effect on aerosol  
69 nucleation is significant (Loukonen et al., 2010; Xu and Zhang, 2013; Henschel et al., 2014; Zhu  
70 et al., 2014; Henschel et al., 2016).

71           Atmospheric measurements have shown that the presence of dicarboxylic acids, including  
72 succinic acid (SUA), is prevalent in ambient particles (Kawamura and Kaplan, 1987; Decesari et  
73 al., 2000; Legrand et al., 2005; Hsieh et al. 2007; Blower et al., 2013). The effect of dicarboxylic  
74 acids on aerosol nucleation involving SA or base molecules has been recognized in theoretical  
75 studies. Wen and Zhang (2012) showed that dicarboxylic acids promote aerosol nucleation with  
76 other nucleating precursors in two directions via hydrogen bonding to the two carboxylic groups



77 on dicarboxylic acids, which is distinct from monocarboxylic acids. Elm et al. (2014) indicated  
78 that clustering of a single pinic acid with SA molecules leads to closed structures because of no  
79 available sites for additional hydrogen bonding. In addition, Elm et al. (2017) suggested that more  
80 than two carboxylic acid groups are required for a given organic oxidation product to efficiently  
81 stabilize sulfuric-acid contained clusters. The interaction between SUA and dimethylamine (DMA)  
82 is strengthened by hydration via forming aminium carboxylate ion pairs (Xu and Zhang, 2013),  
83 while hydration of oxalic acid-AM cluster is somewhat unfavorable under atmospheric conditions  
84 (Weber et al., 2014). Clearly, the interactions of dicarboxylic acids with other nucleation  
85 precursors depend on the type of dicarboxylic acids and the number of the molecules involved in  
86 clustering. Presently, theoretical studies on the effect of dicarboxylic acids on nucleation from  
87 multi-component systems are lacking (Xu et al., 2010; Xu and Zhang, 2013). In particular, the role  
88 of organic acids as well as their participation in stabilizing larger pre-nucleation clusters of the  
89 SA-ammonia/amine systems needs to be evaluated with the presence of hydration in order to better  
90 understand NPF.

91 In this study, we performed theoretical calculations to evaluate the effect of SUA on  
92 hydrated SA·base clusters. Two base species, ammonia and dimethylamine (DMA), were  
93 considered. The Basin Paving Monte Carlo (BPMP) method was employed to sample stable  
94 cluster conformers, and quantum calculations were performed to predict the thermochemical  
95 properties of the multi-component clusters. Geometric and Topological analyses were carried out  
96 to investigate the binding pattern between SUA and SA·base clusters in the presence of hydration.  
97 The implications of the interaction of SUA with hydrated SA·base clusters for atmospheric NPF  
98 are discussed.

## 99 2. COMPUTATIONAL METHODS



100           The methodology of the BPMP conformational sampling combined with quantum  
101 calculations using density functional theory (DFT) was employed to assess the role of SUA in  
102 clustering of SA with base compounds in the presence of water (Xu and Zhang, 2013). Briefly, the  
103 local energy minima in BPMP simulations was searched by using Amber11 package, and the Basin  
104 Hopping Monte Carlo (BHMC) approach was employed to increase the Monte Carlo transition  
105 probability, which allows the clustering system to escape from the traps of local energy minimum.  
106 Hydration of the clustering system was evaluated by employing the TIP3P model. The geometric  
107 optimization and frequency calculations of the BPMP sampled cluster complexes were further  
108 performed at PW91PW91 level of theory with the basis set 6-311++G(2d, 2p) using Gaussian 09  
109 software package (Frisch et al., 2009). Thermodynamic quantities, such as the electronic energy  
110 ( $\Delta E$  with ZPE), enthalpy ( $\Delta H$ ), and Gibbs free energies ( $\Delta G$ ), were obtained on the basis of  
111 unscaled density functional frequencies at temperature of 298.15 K and pressure of 1 atm. Several  
112 basic cluster systems were also examined at the M06-2X/6-311++G(3df,3pd) level of theory,  
113 which has been suggested to be more reliable in predicting binary/ternary cluster formation (Elm  
114 and Mikkelsen, 2012; Leverentz et al., 2013; Zhang et al., 2017). Comparisons of the free energies  
115 with the two different DFT levels of theories between this study and previous available theoretical  
116 and experimental studies are presented in Table 1. The energies derived at the PW91PW91/6-  
117 311++G(2d, 2p) are consistent with those of the M06-2X/6-311++G(3df,3pd) method, and the  
118 differences between our calculations and previous studies are within 1.6 kcal mol<sup>-1</sup>.

119           Topological analysis on the SA·base clusters with hydration and SUA was performed by  
120 employing the Multifunctional Wavefunction Analyzer (Multiwfn) 3.3.8 program (Lu and Chen,  
121 2012). The topological characteristics at the bond critical points (BCPs) were calculated for  
122 electron density ( $\rho$ ), Laplacian of electron density ( $\Delta\rho$ ), and potential energy density ( $V$ ). Since the



123 electron density is highly correlated to bonding strength (Lane et al., 2013), the potential energy  
124 density is an indicator of hydrogen bond energies (Espinosa et al., 1998). The occurrence of proton  
125 transfer in the clusters was determined using the localized orbital locator (LOL). A high LOL value  
126 denotes greatly localized electrons and indicates the existence of a covalent bond (Lu et al., 2012).  
127 The covalent bond is characterized by a negative  $\Delta\rho$ , while a positive  $\Delta\rho$  is associated with a  
128 hydrogen bond. In addition, a newly formed covalent bond via proton transfer was quantitatively  
129 examined in terms of the bond strength using the Laplacian bond order (LBO) as an indicator (Lu  
130 et al., 2013). Both LOL and LBO were calculated with Multiwfn 3.3.8 program (Lu et al., 2012).

131 The extent, to which clusters are hydrated (or the hydrophilicity of the clusters), is affected  
132 by humidity conditions in the atmosphere (Loukonen et al., 2010; Henschel et al., 2014; Henschel  
133 et al., 2016). To examine the influence of SUA on cluster hydration under different humidity  
134 conditions, the relative hydrate distributions over the number of water molecules contained in  
135 clusters were calculated at different relative humidity (RH) levels. The distribution was calculated  
136 according to Henschel et al. (2014), in which the Gibbs free energies of hydration obtained from  
137 DFT calculations are converted to equilibrium constants for the formation of the respective hydrate  
138 by

$$139 \quad K = e^{\frac{-\Delta G^0}{RT}} \quad (1)$$

140 and the relative hydrate population  $x_n$  of the hydrate containing  $n$  water molecules is determined  
141 by

$$142 \quad x_n = \left(\frac{p(\text{H}_2\text{O})}{p^0}\right)^n x_0 e^{\frac{-\Delta G_n}{RT}} \quad (2)$$

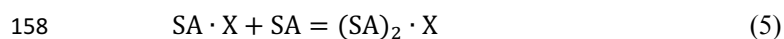
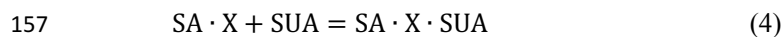
143 where  $p(\text{H}_2\text{O})$  is the water partial pressure,  $p^0$  is the reference pressure (1 atm),  $x_0$  is the population  
144 of the dry cluster chosen so that  $\sum_0^6 x_n = 1$ ,  $T$  is the temperature (298.15 K in this study), and  $R$  is  
145 the molar gas constant.  $p(\text{H}_2\text{O})$  is related to RH through



$$146 \quad p(\text{H}_2\text{O}) = p(\text{H}_2\text{O})_{\text{eq}} \times RH \quad (3)$$

147 where  $p(\text{H}_2\text{O})_{\text{eq}}$  is the water saturation vapor pressure, which is a function of the temperature  
148 following Wexler (Wexler, 1976) Note that only the Gibbs free energy for the single lowest energy  
149 structure for each system of hydration was considered in the calculation, since the Boltzmann  
150 averaging effect over configurations on comparable clusters has been found to be negligible in  
151 most cases, particularly for the free energies of hydration (Erupe et al., 2011; Xu and Zhang, 2013;  
152 Tsona et al., 2015).

153 To assess the importance of uptake of SUA on the SA·base clusters relative to the uptake  
154 of another one SA molecule under atmospheric condition, the ratio in the concentrations  
155 SA·X·SUA to (SA)<sub>2</sub>·X (X denotes either AM or DMA) is calculated assuming equilibrium  
156 conditions,



159 and the equilibrium constants  $K_1$  and  $K_2$  for reactions (4) and (5) are expressed as

$$160 \quad K_1 = \frac{[\text{SA} \cdot \text{X} \cdot \text{SUA}]}{[\text{SA} \cdot \text{X}][\text{SUA}]} = e^{\frac{-\Delta G_1}{RT}} \quad (6)$$

$$161 \quad K_2 = \frac{[(\text{SA})_2 \cdot \text{X}]}{[\text{SA} \cdot \text{X}][\text{SA}]} = e^{\frac{-\Delta G_2}{RT}} \quad (7)$$

162 The concentration ratio between SA·X·SUA and (SA)<sub>2</sub>·X is derived by dividing  $K_1$  and  $K_2$  and the  
163 transformation,

$$164 \quad \frac{[\text{SA} \cdot \text{X} \cdot \text{SUA}]}{[(\text{SA})_2 \cdot \text{X}]} = \frac{[\text{SUA}]}{[\text{SA}]} e^{\frac{-\Delta(\Delta G)}{RT}} \quad (8)$$

165 where  $\Delta(\Delta G)$  is the difference in the Gibbs free energy between reactions (4) and (5) at 298 K.  
166 The ambient concentration of SUA detected at Los Angeles is about  $10^7$  molecules  $\text{cm}^{-3}$   
167 (Kawamura and Kaplan, 1987), and the typical concentration of organic acids in the atmosphere



168 is about  $10^8$ – $10^9$  molecules  $\text{cm}^{-3}$  (Zhang et al., 2015). Also, a lower limit of concentration for  
169 sulfuric acid in promoting NPF in the atmosphere is about  $10^5$  molecules  $\text{cm}^{-3}$  (Zhang et al., 2012).  
170 Hence, the ratio of SA·X·SUA to (SA)<sub>2</sub>·X was expressed on the basis of eq. (8) with the SUA/SA  
171 ratio ranging from 1 to 10, 000, considering the lower limit of the concentration of SA and  
172 available SUA in the atmosphere.

### 173 3. RESULTS AND DISCUSSION

#### 174 3.1 STRUCTURES AND TOPOLOGY

175 The most stable structures (in terms of  $\Delta G$  at  $T=298.15\text{K}$  and  $p=1$  atm) of the hydrated  
176 SA·base clusters are shown in Figures 1-3. Addition of SUA to hydrated SA·base clusters alters  
177 the bonding pattern and rearranges the cluster structure, affecting the free energy and stability for  
178 the cluster formation.<sup>15</sup> Proton transfer with added SUA leads to a change in the bonding degree  
179 for each precursor molecule. Figure 1a shows the absence of proton transfer in the SA·AM cluster,  
180 consistent with the previous studies (Kurtén et al., 2006; Loukonen et al., 2010; Henschel et al.,  
181 2014). When adding SUA to the cluster, proton transfer occurs (Figure 1b), which is confirmed by  
182 the relocation of the LOL high value (Figure 4a). For the SA·AM cluster, a large value of LOL is  
183 adjacent to the SA molecule, indicating that electrons attained to the hydrogen atom (H1) on the  
184 S-O-H group are localized on the SA molecule side. In contrast, a large LOL region is located near  
185 the nitrogen atom (N1) on the AM molecule with the addition of SUA, suggesting that electrons  
186 are greatly localized on the AM side and proton transfer occurs. Because of the proton transfer,  
187 the hydrogen bonding of N1-H1 is converted to a covalent bond, leading to the formation of  
188 ammonium bisulfate. The existence of the new covalent bond is denoted by the available LBO  
189 calculation, showing the bond order of the N1-H1 covalent bond with a value of 0.464. The  
190 formation of the covalent bond is also confirmed by the negative sign of  $\nabla\rho$  at BCP of N1-H1 bond



191 (Table S1). Along with the proton transfer, the electron density (potential energy density) at BCP  
192 of the N1-H1 bond exhibits a significant increase (decrease), from 0.091 (-0.087) a.u. in the  
193 SA·AM cluster to 0.271 (-0.424) a.u. in the SA·AM·SUA cluster. The structures of SA·AM and  
194 SA·DMA hydrates with up to five water molecules in our calculations are consistent with Henschel  
195 et al. (2014). The interactions between SA and AM/DMA in the presence of hydration have been  
196 explored (DePalma et al., 2012; Yu et al., 2012; Qiu et al., 2013; Xu and Zhang, 2013; Tsona et  
197 al., 2015), showing strong bonding among SA, base compound, and water molecules. Another  
198 recent study on glycolic acid found that addition of one glycolic acid molecule to the SA·AM  
199 cluster does not result in proton transfer, unless a second glycolic acid molecule is added (Zhang  
200 et al., 2017). The different behavior in the SA·AM interaction between glycolic acid and SUA is  
201 attributed to the different functional groups in the two organic acids. Hence, SUA is more efficient  
202 than glycolic acid to stabilize the SA·AM clusters.

203 In contrast to the SA·AM cluster, proton transfer occurs for the SA·DMA cluster without  
204 water or SUA (Figures 2 and 4b), because of stronger basicity of DMA than AM (Anderson et al.,  
205 2008). Similarly, proton transfer occurs for the SA·AM·DMA cluster, leading to the formation of  
206 the aminium bisulfate ( $\text{HSO}_4^-$ ) ion pair. Addition of SUA to the SA·DMA·AM·(W)<sub>n</sub> system results  
207 in additional proton transfer between the bisulfate ion and the AM molecule, leading to the  
208 formation of sulfate double-ions ( $\text{SO}_4^{2-}$ ) (Figures 3 and 4c).

209 The dependence of the number of proton transfers on the hydration level is summarized in  
210 Table 3. The hydrations of SA clusters by Xu and Zhang (2013), who employed a similar method  
211 for the structure sampling and quantum calculations, are also included for comparison. It is evident  
212 from Table 3 that both hydration and addition of SUA promote the proton transfer in the SA·base  
213 clusters. Previous studies have identified facile proton transfer by hydration (Ding et al., 2003; Al



214 Natsheh et al., 2004; Loukonen et al., 2010; Xu and Zhang, 2013), and the dependence of proton  
215 transfer on the hydration level has also been suggested by Tsona et al. (2015). For the SA cluster  
216 system, Xu and Zhang (2013) found that proton transfer in the hydrated SA clusters only occurs  
217 with more than two water molecules. In our study, proton transfer occurs when the SA·AM and  
218 the SA·AM·DMA·(W)<sub>5</sub> clusters are hydrated with one more water molecule (Figures 1a and 3a).  
219 The formation of the covalent bond in the monohydrate of SA·AM and the sixth hydrate of  
220 SA·AM·DMA is confirmed by the LOL relocation in Figure S1. Loukonen et al. (2010) also found  
221 that proton transfer occurs in the SA·AM system for the hydrated cluster with two water molecules.  
222 Our results show that neither water molecules nor SUA induce the second proton transfer in  
223 SA·DMA clusters. In contrast, Loukonon et al. (2010) showed that the second proton transfer  
224 occurs when the SA·DMA cluster is hydrated with five water molecules. The different behaviors  
225 for proton transfer with hydration between this study and Loukonen et al. are attributable to the  
226 different sampling methodology used to obtain the most stable conformers of the clusters. Note  
227 that the findings of Loukonen et al. are also in contrast to those by Henschel et al. (2014)

228 Table 4 summarizes the available LBO values for the covalent bonds in the SA·base  
229 clusters with hydration. The dependence of LBO on the cluster hydration level varies with the  
230 clustering systems containing different components. For SA·AM system without SUA, additional  
231 water molecules result in higher LBO of N1-H1 bonds, while for SA·DMA LBO of the N2-H2  
232 bond generally increases at all hydration levels except for the dihydrate. With addition of SUA to  
233 the SA·AM and SA·DMA systems, the LBO values of the pre-existing covalent bonds of SUA-  
234 contained clusters are higher than those of the clusters without SUA at all hydration levels except  
235 for the sixth hydration. This indicates that, although addition of SUA to the two hydrated cluster  
236 systems does not result in additional proton transfer, the presence of SUA enhances the strength



237 of the covalent bonds formed for the initial hydration. Consistently, the electron densities (the  
238 potential energy densities) at BCPs of the N-H bonds are somewhat higher (lower) in the SUA-  
239 containing clusters than in those without SUA for most hydration cases (Tables S2 and S3).

240         Addition of SUA to the SA·base cluster results in cleavage of the original strong hydrogen  
241 bond between the base and SA molecules (Figures 1b, 2b and 3b). As the number of water  
242 molecules increases, the number of possible bonds among the molecules increases, leading to  
243 complicated structures. Note that the carbon chain of SUA tends to bend accordingly as the  
244 hydration degree increases, because both carboxylic groups at the two ends of the carbon chain in  
245 SUA are involved in hydrogen bonding. While the bending of the carbon chain facilitates hydrogen  
246 bonding and stabilizes the clusters, such bending also induces steric hindrance, which partially  
247 cancels out the energy due to additional hydrogen bonding. As expected, the number of hydrogen  
248 bonds attained by the AM molecule in SA·AM·SUA clusters increases with the hydration degree,  
249 which is always equal or larger than that of the corresponding clusters without SUA. The number  
250 of hydrogen bonds formed on AM molecule is closely related to the values of free energy changes  
251 induced by addition of SUA to SA·AM clusters (see detailed discussions in following section on  
252 the energetics). For all DMA-containing clusters, the nitrogen atom of DMA is saturated by two  
253 hydrogen bonds, but the steric hindrance of DMA due to the two free methyl groups likely  
254 corresponds to an important factor that affects the stability of DMA-containing clusters (Ortega et  
255 al., 2012). The complexity of the cluster structures is partially ascribed to the formation of  
256 intramolecular hydrogen bonding in SUA, illustrated by the clusters of SA·AM·SUA·W,  
257 SA·DMA·SUA·W, or SA·AM·DMA·SUA·(W)<sub>5</sub> (Figures 1b, 2b and 3b).



## 258 3.2 ENERGETICS

259 The thermochemical quantities calculated at the PW91PW91/6-311++G(2d, 2p) level of  
260 theory for the most stable cluster configurations are summarized in Table 2. The free energies of  
261 hydration for the clusters, along with the number of water molecules contained in the clusters, are  
262 presented in Figure 5a. The stepwise hydration energies are provided in Table 2. For the hydration  
263 of SA·AM and SA·DMA with up to five water molecules, the hydration free energies calculated  
264 at the PW91PW91/6-311++G(2d, 2p) level are in agreement with those by Henschel et al. (2014)  
265 using the RICC2/aug-cc-pV(T+d)Z level for sulfur and the RICC2/aug-cc-pVTZ level for all other  
266 atoms, but differ from those by Loukonen et al. (2010) at the RI-MP2/aug-cc-pV(T+d)Z level of  
267 theory. Note that some of the structures of the hydrates in this study and the study of Henschel et  
268 al. are different from those of Loukonen et al. (2010), explaining the differences in the energies  
269 among the various studies.

270 Figure 5a shows that addition of one more water molecule to the cluster systems results in  
271 a negative hydration energy relative to the former hydration step at most hydration degrees,  
272 suggesting that hydration overall tends to stabilize the clusters. For SUA-free clusters, the fifth  
273 hydration of SA·AM and SA·DMA·AM and the sixth hydration of SA·DMA exhibit positive or  
274 nearly zero one step hydration free energies. These endergonic steps are ascribed to the SA·base  
275 clusters already being saturated by water molecules in the former hydration steps (Henschel et al.,  
276 2013). For SUA-containing clusters, the addition of one more water molecule at a hydration step  
277 likely leads to a great rise in free energy, resulting in a relatively large positive value of the one  
278 step hydration energy. For example, the one step free energy is 2.99 kcal mol<sup>-1</sup> for the fifth  
279 hydration, 3.24 kcal mol<sup>-1</sup> for the fourth hydration, and 1.32 kcal mol<sup>-1</sup> for the third hydration of  
280 the SA·DMA·AM·SUA cluster. The large increases in free energies for SA·AM·SUA and



281 SA·DMA·SUA clusters are explained by structural rearrangement. The positive one-step  
282 hydration energy for the third hydration of SA·DMA·AM·SUA is likely because the hydrate in  
283 the former step (i.e. the dihydrate) is extraordinarily stable.

284 The relative changes in the free energy due to addition of SUA to the SA·base clusters are  
285 depicted along with hydration degree (Figure 5b). All free energy changes shown in Figure 5b are  
286 negative, confirming that SUA stabilizes the SA·base clusters. For all hydration levels except the  
287 fourth one, the free energy changes for the SA·DMA cluster by SUA addition are more negative  
288 than that for the SA·AM cluster, suggesting that SUA more efficiently stabilizes the hydrated  
289 SA·DMA clusters than the SA·AM cluster. The largest change in the free energy ( $-7.15 \text{ kcal mol}^{-1}$ )  
290 between SA·AM·SUA and SA·AM appears at the fourth hydration step, which is attributable to  
291 the structure change due to SUA addition, i.e., an additional hydrogen bond is formed on the AM  
292 molecule in the fourth hydrate of SA·AM·SUA, while such a hydrogen bond is absent in the  
293 SA·AM cluster until the fifth hydration (Figure 1). The largest negative free energy change ( $-9.86$   
294  $\text{kcal mol}^{-1}$ ) in SA·DMA is under the unhydrated condition. The strong hydrogen bonds between  
295 DMA and the two acids formed in the unhydrated SA·DMA·SUA cluster undergo cleavage due  
296 to water uptake, leading to a smaller free energy difference between the SA·DMA·SUA and  
297 SA·DMA clusters with hydration. In addition, the stabilization effect of hydration on the SA·base  
298 clusters is weakened by addition of SUA, particularly for the SA·DMA and SA·DMA·AM clusters,  
299 with much smaller hydration energies for SA·DMA·SUA and SA·DMA·AM·SUA than the  
300 corresponding clusters without SUA (Fig. 5a). The energetic perturbations by SUA addition are  
301 affected by the hydration degree and the base types, implying synergetic interactions among the  
302 different components in the multi-component clusters.



### 303 3.3 HYDRATION PROFILES

304 The equilibrium hydrate distributions were calculated for the SA·base clusters with and  
305 without the presence of SUA. Figure 6 displays the relative hydrate distributions under three  
306 typical atmospheric RH values, i.e., 20%, 50% and 80%. The SA·base cluster shows a tendency  
307 to be more extensively hydrated with increasing RH, although the different clusters exhibit  
308 variable characteristics in the hydrate distribution.

309 Our results for the SA·AM hydrate distribution are consistent with previous studies  
310 (Loukonen et al., 2010; Henschel et al., 2014), showing that the hydrate distribution of SA·AM is  
311 sensitive to the humidity condition (Figure 6a). The completely dry SA·AM cluster dominates the  
312 hydrate distribution under low RH (<40%), while the trihydrate is most prevalent as RH exceeds  
313 40% because of the strong stability of the trihydrate relative to the monohydrate and dihydrate. In  
314 accordance with the evenly spaced hydration energies, the distribution for hydrated SA·DMA  
315 evenly disperse over the unhydrated cluster to dihydrate (Figure 6b). The unhydrated cluster,  
316 monohydrate, and dihydrate together account for 85% of the total population at all RH levels, and  
317 the peak of the hydrate distribution for SA·DMA shows a continuous shift from the unhydrated  
318 cluster to dihydrate as RH increases. The SA·DMA·AM cluster tends to be dehydrated, as reflected  
319 by the fact that the relative population of dry SA·DMA·AM clusters exceeds 50% even under  
320 highly humid conditions (Figure 6c). This suggests that addition of either DMA or AM  
321 considerably lowers the hydrophilicity of SA·AM or SA·DMA. The dehydration trend of the  
322 SA·DMA·AM cluster is similar to previous investigations,<sup>31</sup> in which the base-containing clusters  
323 with SA were found to be less hydrophilic than the SA clusters.

324 Addition of SUA alters the hydrate distribution of the SA·base clusters. For example, the  
325 hydrate distribution for SA·AM·SUA clusters is slightly broader than that of SA·AM (Figure 6d),



326 with a considerable population of the fourth hydrate for SA·AM·SUA at high RH. Clearly,  
327 addition of SUA promotes hydration of SA·AM. The broad hydrate distribution is consistent with  
328 the more negative hydration energy at the fourth hydration step for SA·AM·SUA clusters relative  
329 to SA·AM. However, the peaks of the distribution for SA·AM·SUA shift with a similar pattern as  
330 SA·AM with varying RH, i.e., bypassing the monohydrate and dihydrate as the most populated  
331 cluster. The hydrate distribution for SA·DMA·SUA shows distinct characteristics for SA·DMA.  
332 In the presence of SUA, over 80% of the clusters exist in a dry state regardless of the humidity  
333 condition (Figure 6e), indicating that hydration of SA·DMA·SUA is less favorable than that of  
334 SA·DMA. The SA·DMA·SUA hydrate distribution peak at the unhydrated cluster is explained  
335 energetically, since addition of SUA greatly reduces the free energy of the dry clusters and the  
336 changes in hydration free energy are relatively small at all hydration levels. The  
337 SA·DMA·AM·SUA clusters are mostly likely dehydrated or hydrated with two water molecules  
338 depending upon the moisture condition (Figure 6f), as the distribution peak shifts between the  
339 unhydrated cluster ( $RH < 70\%$ ) and the dihydrate ( $RH > 70\%$ ). The monohydrate does not exhibit  
340 a maximum of the distribution at any RH level. Clearly, SA·DMA·AM·SUA is more favorably  
341 hydrated compared to SA·DMA·AM.

342 The hydration profiles as functions of RH for the clusters with SA·base are shown in  
343 (Figure 7). Theoretically, the maximal hydration degrees for SA·AM, SA·DMA, and  
344 SA·DMA·AM clusters on average are 2.7, 1.7, and 0.9 of water molecules, respectively, as RH  
345 approaches 100%. The calculations for the hydration of SA·AM and SA·DMA in this study  
346 slightly overestimate the hydration degree, compared to those by Henschel et al. (2014) The  
347 hydrations for SA·AM, SA·AM·SUA, SA·DMA tend to level off at high RH, but such a trend is  
348 not evident for the other three clusters. With SUA, the hydrophilicity of SA·AM and



349 SA·DMA·AM systems is considerably enhanced, implying that more water molecules can be  
350 taken up by SUA-containing clusters. In contrast, the number of water molecules that can be bound  
351 to SA·DMA clusters are greatly reduced if SUA is added to the system, in accordance with that  
352 the most populated cluster of SA·DMA·SUA is unhydrated under different moisture conditions  
353 (Figure 6e).

### 354 3.4 ATMOSPHERIC IMPLICATIONS

355 The formation of SA·base·SUA with addition of one SUA molecule to the SA·base clusters  
356 is energetically favorable (Figure 5b). SUA is more effective than SA to stabilize the SA·base  
357 clusters. In addition to the formation energy, the relative concentration of the precursor species  
358 involved in clustering also governs the cluster distribution in the atmosphere. To evaluate the  
359 importance of SUA in small cluster formation, the concentration ratios of the SA·base clusters  
360 with uptake of SUA to uptake of an additional SA molecule were determined under  
361 atmospherically-relevant concentrations of SUA and SA, along with unhydrated and hydrated SA  
362 clusters. The calculations of the ratios  $[\text{SA}\cdot\text{X}\cdot\text{SUA}]/[(\text{SA})_2\cdot\text{X}]$  (X denotes AM, DMA, water  
363 molecule, or none) are based on the thermochemical data in Table S4, as presented in Table 5.

364 With a high level of SUA, the concentration of SA·AM·SUA cluster is comparable to that  
365 of  $(\text{SA})_2\cdot\text{AM}$ , suggesting that the formation of SA·AM·SUA clusters competes with the formation  
366 of  $(\text{SA})_2\cdot\text{AM}$  in the atmosphere.  $(\text{SA})_2\cdot\text{AM}$  dominates the cluster distribution only if SA and SUA  
367 concentrations are at similar levels. The ratio of SA·AM·SUA to  $(\text{SA})_2\cdot\text{AM}$  is lowered to 1:1000,  
368 when SA concentration is comparable to SUA. SUA-containing clusters are prevalent in the  
369 atmosphere for SA·DMA, since the ratio of  $[\text{SA}\cdot\text{DMA}\cdot\text{SUA}]/[(\text{SA})_2\cdot\text{DMA}]$  reaches as high as  
370 3000:1 with highly abundant SUA.



371 The prevalence of SUA-containing clusters is more significant for the unhydrated SA  
372 clusters and the hydrated SA clusters with one water molecule, with the ratios of  $[\text{SA}\cdot\text{SUA}]/[(\text{SA})_2]$   
373 and  $[\text{SA}\cdot\text{W}\cdot\text{SUA}]/[(\text{SA})_2\cdot\text{W}]$  of higher than  $10^7:1$  and  $10^6:1$ , respectively. Even when the SUA  
374 concentration is relatively low and comparable to SA, the  $[\text{SA}\cdot\text{SUA}]/[(\text{SA})_2]$  and  
375  $[\text{SA}\cdot\text{W}\cdot\text{SUA}]/[(\text{SA})_2\cdot\text{W}]$  ratios are both higher than 500:1. Sulfuric acid dimer has been  
376 recognized as an important precursor for NPF (Zhang et al., 2012), but our study shows that, as  
377 one of most prevalent dicarboxylic acids in atmosphere, SUA inhibits the formation or further  
378 growth of sulfuric acid dimer because of its strong interaction with SA to stabilize the unhydrated  
379 or hydrated SA clusters. This inhibiting effect of SUA on the formation or further growth of  
380 sulfuric acid dimer is more efficient than ketodiperoxy acid (Elm et al., 2016).

381 It should be pointed that steady-state equilibrium for pre-nucleation clusters is rarely  
382 established under atmospheric conditions, because of continuous forward reactions by adding  
383 monomers to form larger clusters during NPF. Hence, the ability whether a cluster grows to form  
384 a nano-sized particle is dependent on the competition between the forward reaction by adding a  
385 monomer and the backward reaction by losing a monomer (evaporation) for each intermediate step.  
386 While the evaporation rate relies on the thermodynamic stability of the cluster, the forward rate  
387 constant is kinetically controlled, dependent on the activation and kinetical energies for the  
388 colliding cluster and monomer. For neutral clusters, electrostatic dipole-dipole interaction likely  
389 plays a key role in reducing the activation barrier. The presence of organic acids typically increases  
390 the dipole moment of clusters (Zhao et al., 2009). We calculated an additional subset of clusters  
391 by adding another sulfuric acid molecule to hydrated  $\text{SA}\cdot\text{DMA}\cdot\text{SUA}$  clusters, i.e.,  
392  $(\text{SA})_2\cdot\text{DMA}\cdot\text{SUA}\cdot(\text{W})_x$ . The stable clusters with two SA molecules are depicted in Figure 8. Table  
393 2 also indicates that the Gibbs energies of  $(\text{SA})_2\cdot\text{DMA}\cdot\text{SUA}\cdot(\text{W})_x$  are negative relative to



394 SA·DMA·SUA·(W)<sub>x</sub>, except for the hydrated form with six H<sub>2</sub>O molecules. These results reveal  
395 that the clusters containing both the base and organic acid are capable of further binding with acid  
396 molecules to promote their growth.

#### 397 4. CONCLUSIONS

398 We have investigated the molecular interactions between SUA and SA·base clusters in the  
399 presence of hydration, including AM and DMA. The stable cluster structures were sampled by the  
400 BPIC approach and further geometric optimization and frequency calculation using quantum  
401 chemical calculations at the PW91PW91/6-311++G(2d, 2p) level. The characteristics of the  
402 structures, thermochemistry, and topology of the clusters were analyzed, focusing on the  
403 differences with and without SUA. In addition, the relative hydrate population and the average  
404 hydration numbers for each SA·base cluster were calculated, and the influence of SUA on the  
405 cluster hydration and the competition between SUA and SA to stabilize the SA·base clusters were  
406 assessed.

407 Addition of SUA to the SA·base cluster systems is energetically favorable at all hydration  
408 levels, suggesting that SUA stabilizes the SA·base clusters and their hydrates. In addition, the  
409 addition of SUA promotes proton transfers in the SA·base clusters. The proton transfer by SUA  
410 addition is confirmed by the formation of new covalent bonds, showing a relocation of the high  
411 LOL value from the SA side to the AM side and a shift from positive to negative for the Laplacian  
412 of electron density. The presence of SUA in SA·AM and SA·DMA clusters generally strengthens  
413 the pre-existing covalent bonds in SA·base·SUA·(W)<sub>n</sub> clusters at the various hydration levels,  
414 since the LBO values of the covalent bonds in SUA-containing clusters are higher than those in  
415 the clusters without SUA. The distribution of hydrate population for SA·AM·SUA is broader than  
416 that for SA·AM. Also, the distribution for SA·DMA·AM·SUA hydrates peaks at the two-water



417 molecule level under elevated RH, but the peak of the distribution for SA·DMA·AM always  
418 corresponds to the unhydrated cluster. The shift in the hydrate distributions to a higher hydration  
419 level in SUA-containing clusters relative to the cluster without SUA suggests that the addition of  
420 SUA enhances the hydrophilicity of SA·AM and SA·DMA·AM. However, the presence of SUA  
421 tends to dehydrate the SA·DMA clusters, since the most prevalent cluster for SA·DMA·SUA is in  
422 a dry state. At equilibrium and considering the typical abundances of SUA and SA in the  
423 atmosphere, the formation of SUA·SA·base (AM or DMA) is comparable to that of (SA)<sub>2</sub>·base.  
424 Hence, the uptake of SUA competes with the uptake of another SA to stabilize the SA·base clusters,  
425 and the presence of SUA hinders the formation and further growth of SA dimer clusters. The  
426 hydrated SA·DMA·SUA cluster is capable of binding with additional acid molecules, which not  
427 only stabilizes the cluster but also promotes its further growth.

428 Our results indicate that the multi-component molecular interaction involving organic acids,  
429 sulfuric acid, and base species promotes NPF in the atmosphere, particularly under polluted  
430 environments because of the co-existence of elevated concentrations of these nucleation precursor  
431 species. Future studies are necessary to assess the kinetics (forward and reverse rates) and potential  
432 energy surface of cluster growth, in order to develop parameterization of NPF for atmospheric  
433 models.

#### 434 **SUPPLEMENTARY MATERIAL**

435 Supplementary material contains additional relief maps for the sulfuric acid-base clusters  
436 and lists of topological properties for the most stable conformers of each cluster categories.

#### 437 **ACKNOWLEDGMENTS**

438 This work was supported by National Natural Science Foundation of China (41675122,  
439 41425015, U1401245, and 41373102), Science and Technology Program of Guangzhou City



440 (201707010188), Team Project from the Natural Science Foundation of Guangdong Province,  
441 China (S2012030006604), Special Program for Applied Research on Super Computation of the  
442 NSFC-Guangdong Joint Fund (the second phase), National Super-computing Centre in  
443 Guangzhou (NSCC-GZ), and Robert A. Welch Foundation (A-1417). The research was partially  
444 conducted with the advanced computing resources provided by Texas A&M High Performance  
445 Research Computing. The authors acknowledged the Laboratory for Molecular Simulations at  
446 Texas A&M University.

447



448

## References

- 449 Andreae, M. O., Rosenfeld, D., Artaxo, P., Costa, A. A., Frank, G. P., Longo, K. M., and Silva-  
450 Dias, M. A. F.: Smoking rain clouds over the Amazon, *Science*, 303, 1337–1342, 2004.
- 451 Al Natsheh, A., Nadykto, A. B., Mikkelsen, K. V., Yu, F., and Ruuskanen, J.: Sulfuric acid and  
452 sulfuric acid hydrates in the gas phase: A DFT investigation, *J. Phys. Chem. A*, 108, 8914–  
453 8929, <https://doi.org/10.1021/jp048858o>, 2004.
- 454 Anderson, K. E., Siepmann, J. I., McMurry, P. H., and VandeVondele, J.: Importance of the  
455 Number of Acid Molecules and the Strength of the Base for Double-Ion Formation in  
456  $(\text{H}_2\text{SO}_4)_m \cdot \text{Base} \cdot (\text{H}_2\text{O})_6$  Clusters, *J. Am. Chem. Soc.*, 130, 14144–14147, <https://doi.org/10.1021/ja8019774>, 2008.
- 458 Bianchi, F., Tröstl, J., Junninen, H., Frege, C., Henne, S., Hoyle, C. R., Molteni, U., Herrmann, E.,  
459 Adamov, A., Bukowiecki, N., Chen, X., Duplissy, J., Gysel, M., Hutterli, M., Kangasluoma,  
460 J., Kontkanen, J., Kürten, A., Manninen, H. E., Münch, S., Peräkylä, O., Petäjä, T., Rondo, L.,  
461 Williamson, C., Weingartner, E., Curtius, J., Worsnop, D. R., Kulmala, M., Dommen, J., and  
462 Baltensperger, U.: New particle formation in the free troposphere: A question of chemistry  
463 and timing, *Science*, 352, 1109–1112, <https://doi.org/10.1126/science.aad5456>, 2016.
- 464 Blower, P. G., Ota, S. T., Valley, N. A., Wood, S. R., and Richmond, G. L.: Sink or Surf:  
465 Atmospheric Implications for Succinic Acid at Aqueous Surfaces, *J. Phys. Chem.* 117, 7887–  
466 7903, <https://doi.org/10.1021/jp405067y>, 2013.
- 467 Cai, R., and Jiang, J.: A new balance formula to estimate new particle formation rate: reevaluating  
468 the effect of coagulation scavenging, *Atmos. Chem. Phys.*, 17, 12659–12675,  
469 <https://doi.org/10.5194/acp-17-12659-2017>, 2017.



- 470 Decesari, S., Facchini, M. C., Fuzzi, S., and Tagliavini, E., Characterization of water-soluble  
471 organic compounds in atmospheric aerosol: A new approach, *J. Geophys. Res. Atmos.*, 105,  
472 1481-1489, <https://doi.org/10.1029/1999JD900950>, 2000.
- 473 DePalma, J. W., Bzdek, B. R., Doren, D. J., and Johnston, M. V.: Structure and energetics of  
474 nanometer size clusters of sulfuric acid with ammonia and dimethylamine, *J. Phys. Chem. A*  
475 116, 1030–1040, <https://doi.org/10.1021/jp210127w>, 2012.
- 476 Ding, C.-G., Laasonen, K., and Laaksonen, A.: Two sulfuric acids in small water clusters, *J. Phys.*  
477 *Chem.* 107, 8648–8658, <https://doi.org/10.1021/jp022575j>, 2003.
- 478 Elm, J., Myllys, N., Luy, J.-N., Kurtén, T., and Vehkamäki, H.: The Effect of Water and Bases on  
479 the Clustering of a Cyclohexene Autoxidation Product C<sub>6</sub>H<sub>8</sub>O<sub>7</sub> with Sulfuric Acid, *J. Phys.*  
480 *Chem.*, 120, 2240–2249, <https://doi.org/10.1021/acs.jpca.6b00677>, 2016.
- 481 Erupe, M. E., Viggiano, A. A., and Lee, S.-H.: The effect of trimethylamine on atmospheric  
482 nucleation involving H<sub>2</sub>SO<sub>4</sub>, *Atmos. Chem. Phys.*, 11, 4767-4775,  
483 <https://doi.org/10.5194/acp-11-4767-2011>, 2011.
- 484 Elm, J., Bilde, M., and Mikkelsen, K. V.: Assessment of density functional theory in predicting  
485 structures and free energies of reaction of atmospheric prenucleation clusters, *J. Chem. Theory*  
486 *and Comp.*, 8, 2071–2077, <https://doi.org/10.1021/ct300192p>, 2012.
- 487 Elm, J., Kurten, T., Bilde, M., and Mikkelsen, K. V.: Molecular interaction of pinic acid with  
488 sulfuric acid: exploring the thermodynamic landscape of cluster growth, *J. Phys. Chem. A*,  
489 118, 7892-7900, <https://doi.org/10.1021/jp503736s> (2014).
- 490 Elm, J., Jen, C. N., Kurtén, T., and Vehkamäki, H.: Strong hydrogen bonded molecular interactions  
491 between atmospheric diamines and sulfuric acid, *J. Phys. Chem.*, 120, 3693–3700,  
492 <https://doi.org/10.1021/acs.jpca.6b03192>, 2016.



- 493 Elm, J., Myllys, N., and Kurtén, T.: What is required for highly oxidized molecules to form clusters  
494 with sulfuric acid? *J. Phys. Chem.*, 121 (23), 4578-4587, doi: 10.1021/acs.jpca.7b03759, 2017.
- 495 Espinosa, E., Molins, E., and Lecomte, C.: Hydrogen bond strengths revealed by topological  
496 analyses of experimentally observed electron densities, *Chem. Phys. Lett.* 285, 170-173,  
497 [https://doi.org/10.1016/S0009-2614\(98\)00036-0](https://doi.org/10.1016/S0009-2614(98)00036-0), 1998.
- 498 Fan, J., Zhang, R., Li, G., and Tao, W.-K.: Effects of aerosols and relative humidity on cumulus  
499 clouds, *J. Geophys. Res.*, 112, D14204, <https://doi.org/10.1029/2006JD008136>, 2007.
- 500 Frisch, M. J., Trucks, G. W., Schlegel, H. B., Scuseria, G. E., Robb, M. A., Cheeseman, J. R.,  
501 Scalmani, G., Barone, V., Petersson, G. A., Nakatsuji, H., Li, X., Caricato, M., Marenich, A.,  
502 Bloino, J., and Janesko, R. G. B. G., Mennucci, B., Hratchian, H. P., Ortiz, J. V., Izmaylov,  
503 A. F., Sonnenberg, J. L., Williams-Young, D., Ding, F., Lipparini, F., Egidi, F., Goings, J.,  
504 Peng, B., Petrone, A., Henderson, T., Ranasinghe, D., Zakrzewski, V. G., Gao, J., Rega, N.,  
505 Zheng, G., Liang, W., Hada, M., Ehara, M., Toyota, K., Fukuda, R., Hasegawa, J., Ishida, M.,  
506 Nakajima, T., Honda, Y., Kitao, O., Nakai, H., Vreven, T., Throssell, K., Montgomery Jr., J.  
507 A., Peralta, J. E., Ogliaro, F., Bearpark, M., Heyd, J. J., Brothers, E., Kudin, K. N., Staroverov,  
508 V. N., Keith, T., Kobayashi, R., Normand, J., Raghavachari, K., Rendell, A., Burant, J. C.,  
509 Iyengar, S. S., Tomasi, J., Cossi, M., Millam, J. M., Klene, M., Adamo, C., Cammi, R.,  
510 Ochterski, J. W., Martin, K. R. L., Morokuma, Farkas, O., Foresman, J. B., and Fox, D. J.:  
511 *Gaussian, Gaussian 09, Revision A.02* (Gaussian, Inc., Wallingford CT, 2009),
- 512 Guo, S., Hu, M., Zamora, M. L., Peng, J., Shang, D., Zheng, J., Du, Z., Wu, Z., Shao, M., Zeng,  
513 L., Molina, M.J., and Zhang, R.: Elucidating severe urban haze formation in China, *Proc. Natl.*  
514 *Acad. Sci. USA*, 111, 17373–17378, <https://doi.org/10.1016/10.1073/pnas.1419604111>, 2014.



- 515 Hanson, D. R., and Eisele, F. L.: Acid–base chemical reaction model for nucleation rates in the  
516 polluted atmospheric boundary layer, *J. Geophys. Res. Atmos.*, 107, 18713–18718,  
517 <https://doi.org/10.1073/pnas.1210285109>, 2002.
- 518 Henschel, H., Ortega, I. K., Kupiainen, O., Olenius, T., Kurtén, T., and Vehkamäki, H.: Hydration  
519 of pure and base-Containing sulfuric acid clusters studied by computational chemistry  
520 methods, *AIP Conference Proceedings*, 1527, 218–221, <https://doi.org/10.1063/1.4803243>,  
521 2013.
- 522 Henschel, H., T. Kurtén, and Vehkamäki, H.: Hydration of Atmospherically Relevant Molecular  
523 Clusters: Computational Chemistry and Classical Thermodynamics, *J. Phys. Chem.*, 120,  
524 2599–2611, <https://doi.org/10.1021/jp500712y>, 2016.
- 525 IPCC, *Climate Change 2013: The Physical Science Basis. Contribution of Working Group I to the*  
526 *Fifth Assessment Report of the Intergovernmental Panel on Climate Change* (Cambridge  
527 University Press, Cambridge, United Kingdom and New York, NY, USA:  
528 <http://www.ipcc.ch/report/ar5/wg1/>, 2013),
- 529 Henschel, H., Navarro, J. C., Yli-Juuti, T., Kupiainen-Maatta, O., Olenius, T., Ortega, I. K., Clegg,  
530 S. L., Kurten, T., Riipinen, I., and Vehkamäki, H.: Hydration of atmospherically relevant  
531 molecular clusters: Computational chemistry and classical thermodynamics, *J. Phys. Chem.*  
532 *A*, 118, 2599–2611, <https://doi.org/10.1021/jp500712y>, 2014.
- 533 Hsieh, L.-Y., Kuo, S.-C., Chen, C.-L., and Tsai, Y. I.: Origin of Low-molecular-weight  
534 Dicarboxylic Acids and their Concentration and Size Distribution Variation in Suburban  
535 Aerosol, *Atmos. Environ.*, 41, 6648–6661, <https://doi.org/10.1016/j.atmosenv.2007.04.014>  
536 2007.



- 537 Kawamura, K., and Kaplan, I. R.: Motor exhaust emissions as a primary source for dicarboxylic  
538 acids in Los Angeles ambient air, *Environ. Sci. Technol.*, 21, 105-110, 1987. Legrand, M.,  
539 Preunkert, S., Galy-Lacaux, C., Liousse, C., and Wagenbach, D.: *J. Geophys. Res.*:  
540 Atmospheric year-round records of dicarboxylic acids and sulfate at three French sites located  
541 between 630 and 4360 m elevation, *Atmos. 110*, <https://doi.org/10.1029/2004JD005515>, 2005.  
542 Kuang, C., Riipinen, I., Sihto, S.-L., Kulmala, M., McCormick, A. V., and McMurry, P. H.: An  
543 improved criterion for new particle formation in diverse atmospheric environments, *Atmos.*  
544 *Chem. Phys.*, 10, 8469–8480, doi:10.5194/acp-10-8469-2010, 2010.  
545 Kulmala, M. and Kerminen, V. M.: On the formation and growth of atmospheric nanoparticles,  
546 *Atmos. Res.*, 90, 132–150, <https://doi.org/10.1016/j.atmosres.2008.01.005>, 2008.  
547 Kurtén, T., Sundberg, M. R., Vehkamäki, H., Noppel, M., Blomqvist, J., and Kulmala, M.: Ab  
548 initio and density functional theory reinvestigation of gas-phase sulfuric acid monohydrate  
549 and ammonium hydrogen sulfate, *J. Phys. Chem.* <https://doi.org/110>, 7178–7188,  
550 10.1021/jp0613081, 2006.  
551 Lane, J. R., Contreras-García, J., Piquemal, J.-P., Miller, B. J., and Kjaergaard, H. G.: Are bond  
552 critical points really critical for hydrogen bonding? *J. Chem. Theory and Comp.* 9, 3263–3266,  
553 <https://doi.org/10.1021/ct400420r>, 2013.  
554 Lee, S. H., Reeves, J. M., Wilson, J. C., Hunton, D. E., Viggiano, A. A., Miller, T. M., Ballenthin,  
555 J. O., and Lait, L. R.: Particle formation by ion nucleation in the upper troposphere and lower  
556 stratosphere: *Science*, 301, 1886–1889, <https://doi.org/10.1126/science.1087236>, 2003.  
557 Leverentz, H. R., Siepmann, J. I., Truhlar, D. G., Loukonen, V., and Vehkamäki, H.: Energetics  
558 of atmospherically implicated clusters made of sulfuric acid, ammonia, and dimethyl amine,  
559 *J. Phys. Chem. A*, 117, 3819–3825, <https://doi.org/10.1021/jp402346u>, 2013.



- 560 Li, G., Wang, Y., and Zhang, R.: Implementation of a two-moment bulk microphysics scheme to  
561 the WRF model to investigate aerosol-cloud interaction, *J. Geophys. Res.* 113, D15211,  
562 <https://doi.org/10.1029/2007JD009361>, 2008.
- 563 Loukonen, V., Kurtén, T., Ortega, I. K., Vehkamäki, H., Pádua, A. A. H., Sellegri, K., Kulmala,  
564 M.: Enhancing effect of dimethylamine in sulfuric acid nucleation in the presence of water –  
565 a computational study, *Atmos. Chem. Phys.*, 10, 4961-4974, <https://doi.org/10.5194/acp-10-4961-2010>, 2010.
- 567 Lu, T., and Chen, F.: Multiwfn: A multifunctional wavefunction analyzer, *J. Comput. Chem.* 33,  
568 580-592, <https://doi.org/10.1002/jcc.22885>, 2012.
- 569 Lu, T., and Chen, F.: Bond order analysis based on the Laplacian of electron density in fuzzy  
570 overlap space, *J. Phys. Chem. A*, 117, 3100–3108, <https://doi.org/10.1021/jp4010345>, 2013.
- 571 McGraw, R., and Zhang, R.: Multivariate analysis of homogeneous nucleation rate measurements:  
572 I. Nucleation in the p-toluic acid/sulfuric acid/water system, *J. Chem. Phys.* 128, 064508,  
573 <https://doi.org/10.1063/1.2830030>, 2008.
- 574 Merikanto, J., Spracklen, D. V., Mann, G. W., Pickering, S. J., and Carslaw, K. S.: Impact of  
575 nucleation on global CCN, *Atmos. Chem. Phys.*, 9, 8601-8616, <https://doi.org/10.5194/acp-9-8601-2009>, 2009.
- 577 Nadykto, A. B., and Yu, F.: Strong hydrogen bonding between atmospheric nucleation precursors  
578 and common organics, *Chem. Phys. Lett.*, 435, 14-18,  
579 <https://doi.org/10.1016/j.cplett.2006.12.050>, 2007.
- 580 Nadykto, A.B., Yu, F., Jakovleva, M.V., Herb, J., and Xu, Y.: Amines in the Earth's Atmosphere:  
581 A Density Functional Theory Study of the Thermochemistry of Pre-Nucleation Clusters,  
582 *Entropy*, 13, 554–569, <https://doi.org/10.3390/e13020554>, 2011.



- 583 Ortega, I. K., Kupiainen, O., Kurtén, T., Olenius, T., Wilkman, O., McGrath, M. J., Loukonen, V.,  
584 and Vehkamäki, H.: From quantum chemical formation free energies to evaporation rates,  
585 Atmos. Chem. Phys., 12, 225-235, <https://doi.org/10.5194/acp-12-225-2012>, 2012
- 586 Riccobono, F., Schobesberger, S., Scott, C. E., Dommen, J., Ortega, I. K., Rondo, L., Almeida, J.,  
587 Amorim, A., Bianchi, F., Breitenlechner, M., David, A., Downard, A., Dunne, E. M., Duplissy,  
588 J., Ehrhart, S., Flagan, R. C., Franchin, A., Hansel, A., Junninen, H., Kajos, M., Keskinen,  
589 H., Kupc, A., Kürten, A., Kvashin, A. N., Laaksonen, A., Lehtipalo, K., Makhmutov, V.,  
590 Mathot, S., Nieminen, T., Onnela, A., Petäjä, T., Praplan, A. P., Santos, F. D., Schallhart, S.,  
591 Seinfeld, J. H., Sipilä, M., Spracklen, D. V., Stozhkov, Y., Stratmann, F., Tomé, A.,  
592 Tsagkogeorgas, G., Vaattovaara, P., Viisanen, Y., Vrtala, A., Wagner, P. E., Weingartner,  
593 E., Wex, H., Wimmer, D., Carslaw, K. S., Curtius, J., Donahue, N. M., Kirkby, J., Kulmala,  
594 M., Worsnop, D. R., and Baltensperger, U.: Oxidation products of biogenic emissions  
595 contribute to nucleation of atmospheric particles, Science 344, 717-721,  
596 <https://doi.org/10.1126/science.1243527>, 2014.
- 597 Qiu, C., and Zhang, R.: Multiphase chemistry of atmospheric amines, Phys. Chem. Chem. Phys.,  
598 15, 5738-5752, <https://doi.org/10.1039/C3CP43446J>, 2013.
- 599 Tröstl, J., Chuang, W. K., Gordon, H., Heinritzi, M., Yan, C., Molteni, U., Ahlm, L., Frege, C.,  
600 Bianchi, F., Wagner, R., Simon, M., Lehtipalo, K., Williamson, C., Craven, J. S., Duplissy,  
601 J., Adamov, A., Almeida, J., Bernhammer, A.-K., Breitenlechner, M., Brilke, S., Dias, A.,  
602 Ehrhart, S., Flagan, R. C., Franchin, A., Fuchs, C., Guida, R., Gysel, M., Hansel, A., Hoyle,  
603 C. R., Jokinen, T., Junninen, H., Kangasluoma, J., Keskinen, H., Kim, J., Krapf, M., Kürten,  
604 A., Laaksonen, A., Lawler, M., Leiminger, M., Mathot, S., Möhler, O., Nieminen, T., On-  
605 nelä, A., Petäjä, T., Piel, F. M., Miettinen, P., Rissanen, M. P., Rondo, L., Sarnela, N.,



- 606 Schobesberger, S., Sengupta, K., Sipilä, M., Smith, J. N., Steiner, G., Tomè, A., Virtanen,  
607 A., Wagner, A. C., Weingartner, E., Wimmer, D., Winkler, P. M., Ye, P., Carslaw, K. S.,  
608 Curtius, J., Dommen, J., Kirkby, J., Kulmala, M., Riipinen, I., Worsnop, D. R., Donahue, N.  
609 M., and Baltensperger, U.: The role of low-volatility organic compounds in initial particle  
610 growth in the atmosphere, *Nature*, 533, 527–531, <https://doi.org/10.1038/nature18271>, 2016.
- 611 Tsona, N. T., Henschel, H., Bork, N., Loukonen, V., and Vehkamäki, H.: Structures, Hydration,  
612 and Electrical Mobilities of Bisulfate Ion–Sulfuric Acid–Ammonia/Dimethylamine Clusters:  
613 A Computational Study, *J. Phys. Chem. A*, 119, 9670–9679,  
614 <https://doi.org/10.1021/acs.jpca.5b03030>, 2015.
- 615 Wang, L., Khalizov, A.F., Zheng, J., Xu, W., Lal, V., Ma, Y., and Zhang, R.: Atmospheric  
616 nanoparticles formed from heterogeneous reactions of organics, *Nature Geosci.*, 3, 238–242,  
617 <https://doi.org/10.1038/ngeo778>, 2010.
- 618 Wang, J., Krejci, R., Giangrande, S., Kuang, C., Barbosa, H. M. J., Brito, J., Carbone, S., Chi, X.,  
619 Comstock, J., Ditas, F., Lavric, J., Manninen, H. E., Mei, F., Moran-Zuloaga, D., Pöhlker, C.,  
620 Pöhlker, M. L., Saturno, J., Schmid, B., Souza, R. A. F., Springston, S. R., Tomlinson, J. M.,  
621 Toto, T., Walter, D., Wimmer, D., Smith, J. N., Kulmala, M., Machado, L. A. T., Artaxo, P.,  
622 Andreae, M. O., Petäjä, T., and Martin, S. T.: Amazon boundary layer aerosol concentration  
623 sustained by vertical transport during rainfall, *Nature*, 539, 416–419,  
624 <https://doi.org/10.1038/nature19819>, 2016.
- 625 Wang, C.-Y., Jiang, S., Liu, Y.-R., Wen, H., Wang, Z.-Q., Han, Y.-J., Huang, T., Huang, W.:  
626 Synergistic Effect of Ammonia and Methylamine on Nucleation in the Earth's Atmosphere.  
627 A Theoretical Study, *J. Phys. Chem. A*, 122, 3470–3479, <https://doi.org/10.1021/acs.jpca.8b0068>, 2018.
- 628



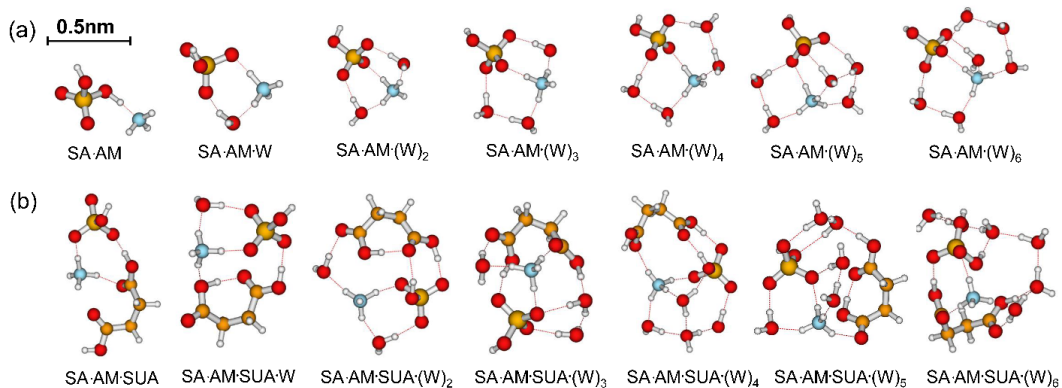
- 629 Weber, K. H., Liu, Q., and Tao, F.-M.: Theoretical study on stable small clusters of oxalic acid  
630 with ammonia and water, *J. Phys. Chem. A*, 118, 1451-1468,  
631 <https://doi.org/10.1021/jp4128226>, 2014.
- 632 Wexler, A.: Vapor pressure formulation for water in range 0 to 100 C. A revision, *J. Res. Nat. Bur.*  
633 *Stand.* 80A, 775-785, 1976.
- 634 Xu, Y., Nadykto, A. B., Yu, F., Jiang, L., and Wang, W.: Formation and properties of hydrogen-  
635 bonded complexes of common organic oxalic acid with atmospheric nucleation precursors, *J.*  
636 *Mol. Struct.: THEOCHEM*, 951, 28-33, <https://doi.org/10.1016/j.theochem.2010.04.004>,  
637 2010a.
- 638 Xu, Y., Nadykto, A. B., Yu, F., Herb, J., and Wang, W.: Interaction between common organic  
639 acids and trace nucleation species in the Earth's atmosphere, *J. Phys. Chem. A*, 114, 387-96,  
640 <https://doi.org/10.1021/jp9068575>, 2010b.
- 641 Xu, W., and Zhang, R.: Theoretical investigation of interaction of dicarboxylic acids with common  
642 aerosol nucleation precursors, *J. Phys. Chem.*, 116, 4539-4550, [https://doi.org/](https://doi.org/10.1021/jp301964u)  
643 [10.1021/jp301964u](https://doi.org/10.1021/jp301964u), 2012.
- 644 Xu, W., and Zhang, R.: A theoretical study of hydrated molecular clusters of amines and  
645 dicarboxylic acids, *J. Chem. Phys.*, 139, 064312, <https://doi.org/10.1063/1.4817497>, 2013.
- 646 Xu, W., Gomez-Hernandez, M., Guo, S., Secret, J., Marrero-Ortiz, W., Zhang, A. L., and Zhang,  
647 R.: Acid-catalyzed reactions of epoxides for atmospheric nanoparticle growth, *J. Am. Chem.*  
648 *Soc.*, 136, 15477–15480, <https://doi.org/10.1021/ja508989a>, 2014.
- 649 Yu, H., McGraw, R., and Lee, S.-H.: Effects of amines on formation of sub-3 nm particles and  
650 their subsequent growth, *Geophys. Res. Lett.*, 39, L02807,  
651 <https://doi.org/10.1029/2011GL050099>, 2012.



- 652 Yue, D. L., Hu, M., Zhang, R. Y., Wang, Z. B., Zheng, J., Wu, Z. J., Wiedensohler, A., He, L. Y.,  
653 Huang, X. F., and Zhu, T.: The roles of sulfuric acid in new particle formation and growth in  
654 the mega-city of Beijing, *Atmos. Chem. Phys.* 10, 4953–4960, [https://doi.org/10.5194/acp-](https://doi.org/10.5194/acp-10-4953-2010)  
655 10-4953-2010, 2010.
- 656 Yue, D. L., Hu, M., Zhang, R. Y., Wu, Z. J., Su, H., Wang, Z. B., and Wiedensohler, A.: Potential  
657 contribution of new particle formation to cloud condensation nuclei in Beijing, *Atmos.*  
658 *Environ.*, 45, 6070-6077, <https://doi.org/10.1016/j.atmosenv.2011.07.037>, 2011.
- 659 Yao, L., Garmash, O., Bianchi, F., Zheng, J., Yan, C., Kontkanen, J., Junninen, H., Mazon, B. S.,  
660 Ehn, M., Paasonen, P., Sipila, M., Wang, M., Wang, X., Xiao, S., Chen, H., Lu, Y., Zhang,  
661 B., Wang, D., Fu, Q., Geng, F., Li, L., Wang, H., Qiao, L., Yang, X., Chen, J., Kerminen, V.,  
662 Petaja, T., Worsnop, D., Kulmala, M., Wang, L.: Atmospheric new particle formation from  
663 sulfuric acid and amines in a Chinese megacity, *Science*, 361, 278-281,  
664 <https://doi.org/10.1126/science.aao4839>, 2018.
- 665 Zhang, H., Kupiainen-Määttä, O., Zhang, X., Molinero, V., Zhang, Y., and Li, Z., The  
666 enhancement mechanism of glycolic acid on the formation of atmospheric sulfuric acid–  
667 ammonia molecular clusters, *J. Chem. Phys.*, 146, 184308, <https://doi.org/10.1063/1.4982929>,  
668 2017.
- 669 Zhang, R.: Getting to the critical nucleus of aerosol formation, *Science*, 328, 1366-1367,  
670 <https://doi.org/10.1126/science.1189732>, 2010.
- 671 Zhang, R., Suh, I., Zhao, J., Zhang, D., Fortner, E. C., Tie, X., Molina, L. T., and Molina, M. J.:  
672 Atmospheric new particle formation enhanced by organic acids, *Science*, 304, 1487-1490,  
673 <https://doi.org/10.1126/science.1095139>, 2004.



- 674 Zhang, R., Wang, L., Khalizov, A. F., Zhao, J., Zheng, J., McGraw, R. L., and Molina, L. T.:  
675 Formation of nanoparticles of blue haze enhanced by anthropogenic pollution, Proc. Natl.  
676 Acad. Sci. USA, 106, 17650-17654, <https://doi.org/10.1073/pnas.0910125106>, 2009.
- 677 Zhang, R., Khalizov, A.F., Wang, L., Hu, M., Xu, W.: Nucleation and growth of nanoparticles in  
678 the atmosphere, Chem. Rev., 112, 1957-2011, <https://doi.org/10.1021/cr2001756>, 2012.
- 679 Zhang, R., Wang, G., Guo, S., Zamora, M. L., Ying, Q., Lin, Y., Wang, W., Hu, M., and Wang Y.:  
680 Formation of urban fine particulate matter, Chem. Rev., 115, 3803-3855,  
681 <https://doi.org/10.1021/acs.chemrev.5b00067>, 2015.
- 682 Zhao, J., Khalizov, A., Zhang, R., and McGraw, R.: Hydrogen bonding interaction of molecular  
683 complexes and clusters of aerosol nucleation precursors, J. Phys. Chem. A 113, 680–689,  
684 <https://doi.org/10.1021/jp806693r>, 2009.
- 685 Zhu, Y. P., Liu, Y. R., Huang, T., Jiang, S., Xu, K. M., Wen, H., Zhang, W. J., and Huang, W.:  
686 Theoretical study of the hydration of atmospheric nucleation precursors with acetic acidJ,  
687 Phys. Chem. A, 118, 7959-7974, <https://doi.org/10.1021/jp506226z>, 2014.
- 688



689

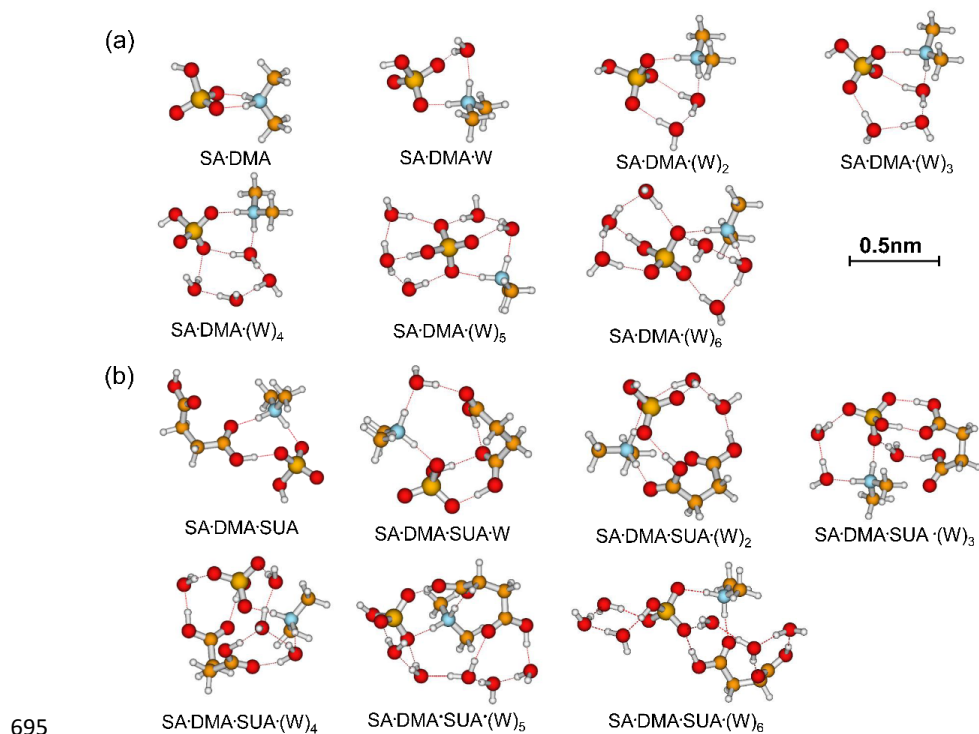
690 FIG. 1. Most stable configurations of the hydrated SA•AM clusters and the clusters with one

691 SUA addition. The hydration is with 0-6 water molecules. The sulfur (carbon) atoms are depicted

692 as large (small) yellow balls, oxygen atoms in red, nitrogen atoms in blue, and hydrogen atoms

693 in white. The dash line denotes the hydrogen bond.

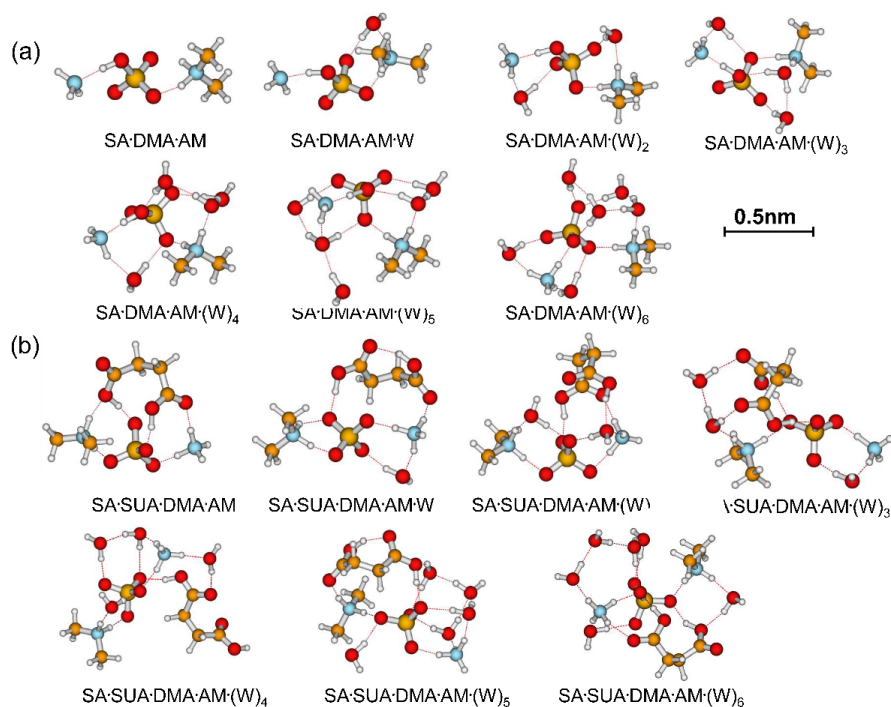
694



696 FIG. 2. Most stable configurations of the hydrated SA•DMA clusters and the clusters with one  
697 SUA addition. The hydration is with 0-6 water molecules.

698

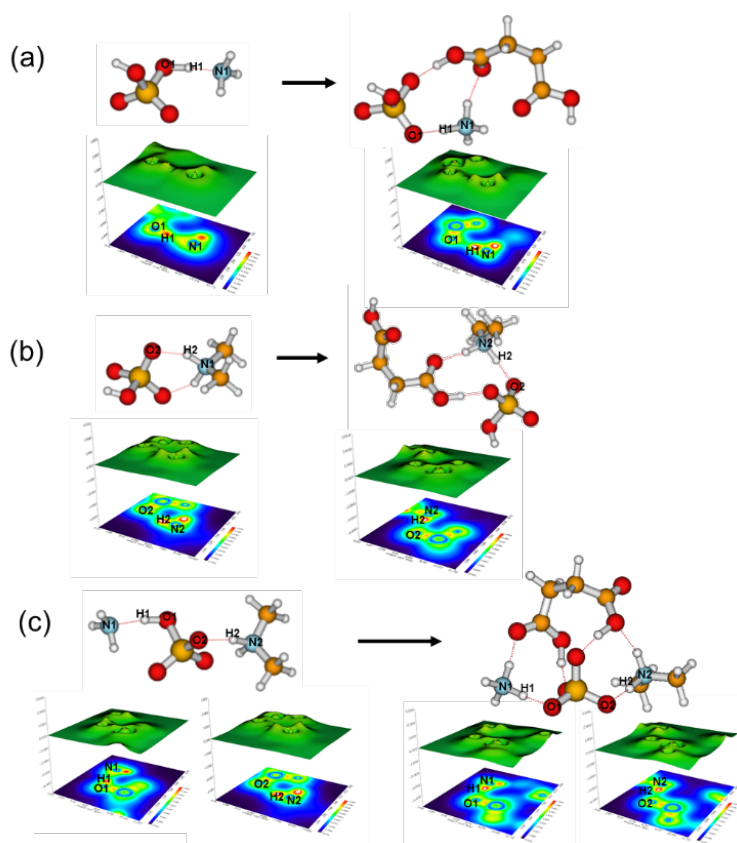
699



700

701 FIG. 3. Most stable configurations of the hydrated SA•DMA•AM clusters and the clusters with  
702 one SUA addition. The hydration is with 0-6 water molecules.

703



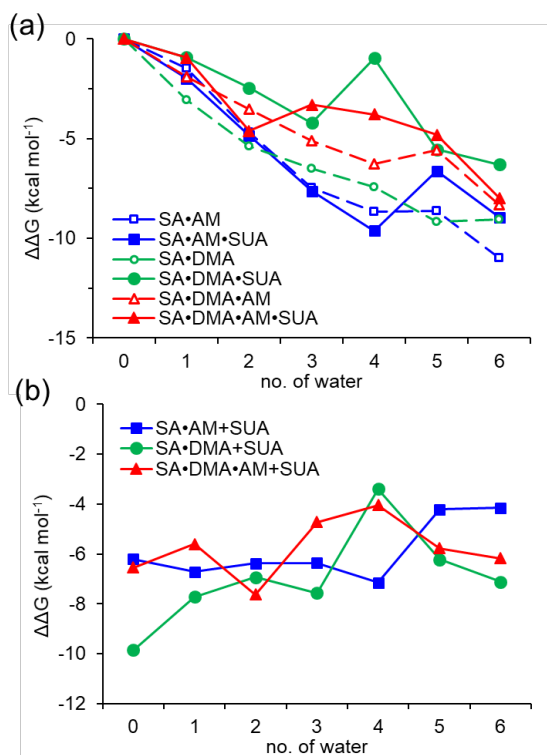
704

705 FIG. 4. Relief maps with the projection of localized orbital locator for clusters of (a) SA·AM and  
706 SA·AM·SUA, (b) SA·DMA, SA·DMA·SUA, and (c) SA·DMA·AM and SA·DMA·AM·SUA.

707 Hydrogen bonds are shown as dashed lines. A large LOL value reflects that electrons are greatly  
708 localized, indicating the existence of a covalent bond.

709

710



711

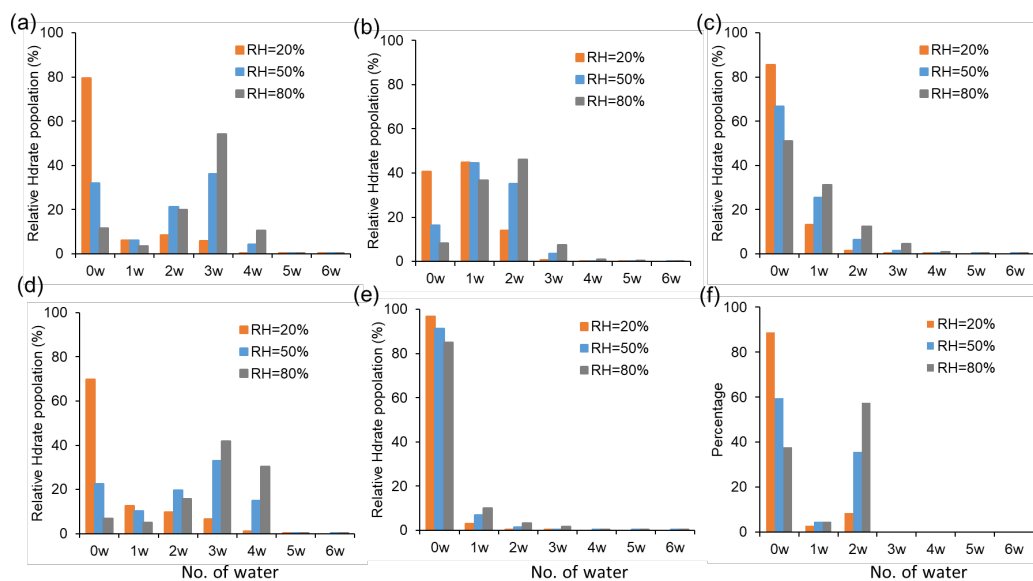
712 FIG. 5. Hydration free energies (a) and the relative Gibbs free energy changes due to addition of

713 one SUA molecule to SA•base clusters (b) at  $T=298.15$  K and  $p=1$  atm. The free energy is

714 calculated at the PW91PW91/6-311++G(2d, 2p) level.

715

716



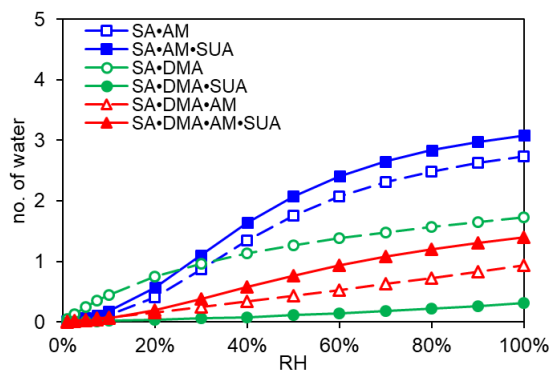
717

718 FIG. 6. Hydrate distributions of clusters under different RH levels (20%, 50% and 80%). (a), (b),

719 and (c) are clusters for SA•AM, SA•DMA, and SA•DMA•AM, respectively. (d), (e) and (f) are

720 clusters with one SUA addition on the basis of (a), (b) and (c) clusters. In all RH cases,  $T=298$  K.

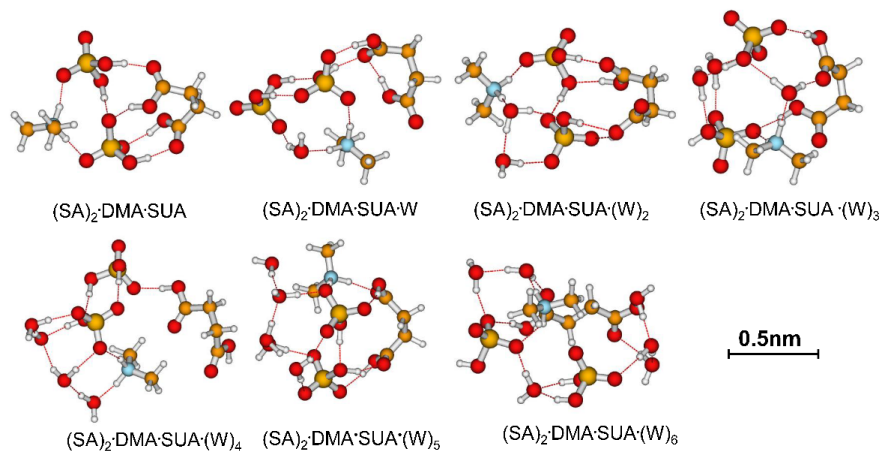
721



722

723 FIG. 7. Average hydration numbers per cluster for various SA-base clusters at 298.15 K.

724



725

726 FIG. 8. Most stable configurations of the hydrated (SA)<sub>2</sub>•DMA•SUA clusters. The hydration is

727 with 0-6 water molecules (W).

728

729



730 Table 1. Theoretical and experimental values of the free energy change for several basic  
 731 reactions in kcal mol<sup>-1</sup>.

Reactions	This study		refs
	PW91PW91/6- 311++G(2df,2pd)	M06-2X/6- 311++G(3df,3pd)	
SA+AM → SA•AM	-7.65	-8.00	-8.5 <sup>a,*</sup> , -7.77 <sup>b</sup> , -6.64 <sup>c</sup> , -7.84 <sup>d</sup>
SA+DMA → SA•DMA	-11.13	-11.24	13.66 <sup>c</sup> , 11.38 <sup>c</sup>
SA•AM+W → SA•AM•W	-1.48	-0.07	-1.41 <sup>b</sup> , -1.67 <sup>f</sup>
SA•DMA+W → SA•DMA•W	-3.06	-3.63	-3.67 <sup>e</sup> , -2.89 <sup>f</sup>
SA•AM+SUA → SA•AM•SUA	-6.20	-7.29	-
SA•DMA+SUA → SA•DMA•SUA	-9.86	-11.46	-

732 <sup>a</sup> From Hanson and Eisele (2002)

733 <sup>b</sup> From Nadykto and Yu (2007)

734 <sup>c</sup> From Kurtén et al. (2008)

735 <sup>d</sup> From Elm et al. (2012)

736 <sup>e</sup> From Nadykto et al. (2011)

737 <sup>f</sup> From Henschel et al. (2014)

738 \* corresponds to experimental results.

739



740 Table 2. Calculated binding energy  $\Delta E(\text{ZPE})$ , enthalpy  $\Delta H$ , and Gibbs free energy  $\Delta G$  (at  
 741  $T=298.15$  K and  $p=1$  atm) at the PW91PW91/6-311++G(2d, 2p) level of theory for the hydrated  
 742 clusters. Energies are in kcal mol<sup>-1</sup>.

Reactions	$\Delta E(\text{ZPE})$	$\Delta H$	$\Delta G$
SA+AM → SA•AM	-15.95	-16.51	-7.65
SA+AM+W → SA•AM•W	-26.40	-28.02	-9.13
SA+AM+2W → SA•AM•(W) <sub>2</sub>	-39.14	-41.58	-12.33
SA+AM+3W → SA•AM•(W) <sub>3</sub>	-49.96	-52.98	-15.11
SA+AM+4W → SA•AM•(W) <sub>4</sub>	-59.63	-63.30	-16.32
SA+AM+5W → SA•AM•(W) <sub>5</sub>	-69.20	-73.58	-16.26
SA+AM+6W → SA•AM•(W) <sub>6</sub>	-78.71	-83.37	-18.64
SA+DMA → SA•DMA	-21.16	-21.11	-11.13
SA+DMA+W → SA•DMA•W	-33.46	-34.13	-14.19
SA+DMA+2W → SA•DMA•(W) <sub>2</sub>	-45.02	-46.60	-16.51
SA+DMA+3W → SA•DMA•(W) <sub>3</sub>	-54.37	-56.57	-17.62
SA+DMA+4W → SA•DMA•(W) <sub>4</sub>	-62.47	-65.25	-18.56
SA+DMA+5W → SA•DMA•(W) <sub>5</sub>	-75.68	-79.92	-20.31
SA+DMA+6W → SA•DMA•(W) <sub>6</sub>	-84.43	-89.24	-20.16
SA+SUA+AM → SA•SUA•AM	-34.19	-34.69	-13.85
SA+SUA+AM+W → SA•SUA•AM•W	-45.65	-47.18	-15.85
SA+SUA+AM+2W → SA•SUA•AM•(W) <sub>2</sub>	-58.95	-61.44	-18.70
SA+SUA+AM+3W → SA•SUA•AM•(W) <sub>3</sub>	-70.41	-73.52	-21.47
SA+SUA+AM+4W → SA•SUA•AM•(W) <sub>4</sub>	-80.92	-84.95	-23.47
SA+SUA+AM+5W → SA•SUA•AM•(W) <sub>5</sub>	-86.75	-90.96	-20.48
SA+SUA+AM+6W → SA•SUA•AM•(W) <sub>6</sub>	-98.52	-104.27	-22.80
SA+SUA+DMA → SA•SUA•DMA	-42.01	-41.42	-20.98
SA+SUA+DMA+W → SA•SUA•DMA•W	-54.80	-55.47	-21.92
SA+SUA+DMA+2W → SA•SUA•DMA•(W) <sub>2</sub>	-64.86	-66.03	-23.45
SA+SUA+DMA+3W → SA•SUA•DMA•(W) <sub>3</sub>	-75.90	-78.21	-25.19
SA+SUA+DMA+4W → SA•SUA•DMA•(W) <sub>4</sub>	-82.83	-86.21	-21.95
SA+SUA+DMA+5W → SA•SUA•DMA•(W) <sub>5</sub>	-92.80	-96.19	-26.54
SA+SUA+DMA+6W → SA•SUA•DMA•(W) <sub>6</sub>	-103.04	-107.49	-27.29
2SA+SUA+DMA → (SA) <sub>2</sub> •SUA•DMA	-62.90	-63.35	-26.12
2SA+SUA+DMA+W → (SA) <sub>2</sub> •SUA•DMA•W	-69.95	-70.90	-25.11
2SA+SUA+DMA+2W → (SA) <sub>2</sub> •SUA•DMA•(W) <sub>2</sub>	-79.07	-80.72	-25.30
2SA+SUA+DMA+3W → (SA) <sub>2</sub> •SUA•DMA•(W) <sub>3</sub>	-91.67	-94.06	-28.71
2SA+SUA+DMA+4W → (SA) <sub>2</sub> •SUA•DMA•(W) <sub>4</sub>	-93.90	-96.57	-24.36
2SA+SUA+DMA+5W → (SA) <sub>2</sub> •SUA•DMA•(W) <sub>5</sub>	-115.58	-120.45	-31.69



$2SA+SUA+DMA+6W \rightarrow (SA)_2 \cdot SUA \cdot DMA \cdot (W)_6$	-108.55	-112.07	-22.50
$SA+DMA+AM \rightarrow SA \cdot DMA \cdot AM$	-23.83	-33.01	-14.15
$SA+DMA+AM+W \rightarrow SA \cdot DMA \cdot AM \cdot W$	-44.15	-45.58	-16.05
$SA+DMA+AM+2W \rightarrow SA \cdot DMA \cdot AM \cdot (W)_2$	-54.34	-56.54	-17.69
$SA+DMA+AM+3W \rightarrow SA \cdot DMA \cdot AM \cdot (W)_3$	-66.01	-69.12	-19.27
$SA+DMA+AM+4W \rightarrow SA \cdot DMA \cdot AM \cdot (W)_4$	-75.88	-79.62	-20.44
$SA+DMA+AM+5W \rightarrow SA \cdot DMA \cdot AM \cdot (W)_5$	-83.63	-87.99	-19.74
$SA+DMA+AM+6W \rightarrow SA \cdot DMA \cdot AM \cdot (W)_6$	-97.07	-102.91	-22.48
$SA+SUA+DMA+AM \rightarrow SA \cdot SUA \cdot DMA \cdot AM$	-54.69	-56.03	-20.69
$SA+SUA+DMA+AM+W \rightarrow SA \cdot SUA \cdot DMA \cdot AM \cdot W$	-62.07	-63.89	-21.65
$SA+SUA+DMA+AM+2W \rightarrow SA \cdot SUA \cdot DMA \cdot AM \cdot (W)_2$	-77.31	-80.08	-25.32
$SA+SUA+DMA+AM+3W \rightarrow SA \cdot SUA \cdot DMA \cdot AM \cdot (W)_3$	-83.64	-87.00	-24.00
$SA+SUA+DMA+AM+4W \rightarrow SA \cdot SUA \cdot DMA \cdot AM \cdot (W)_4$	-92.14	-95.95	-24.48
$SA+SUA+DMA+AM+5W \rightarrow SA \cdot SUA \cdot DMA \cdot AM \cdot (W)_5$	-104.97	-110.11	-25.51
$SA+SUA+DMA+AM+6W \rightarrow SA \cdot SUA \cdot DMA \cdot AM \cdot (W)_6$	-115.86	-121.79	-28.66

743

744



745 Table 3. Number of Proton Transfers within hydrated Clusters (T = 298.15 K).

Cluster	No. of water						
	0	1	2	3	4	5	6
SA <sup>a</sup>	0	0	0	1	1	1	1
SA•AM	0	1	1	1	1	1	1
SA•AM•SUA	1	1	1	1	1	1	1
SA•DMA	1	1	1	1	1	1	1
SA•DMA•SUA	1	1	1	1	1	1	1
SA•DMA•AM	1	1	1	1	1	1	2
SA•DMA•AM•SUA	2	2	2	2	2	2	2

746 <sup>a</sup> From Xu and Zhang (2013)

747



748 Table 4. Laplacian bond order (LBO) of the newly formed covalent bond (nitrogen-hydrogen  
 749 bond) between in the clusters (a.u.).

Clusters	Bonds	No. of water						
		<i>0</i>	<i>1</i>	<i>2</i>	<i>3</i>	<i>4</i>	<i>5</i>	<i>6</i>
SA•AM	N1-H1	-	0.383	0.577	0.586	0.580	0.636	0.663
SA•AM•SUA	N1-H1	0.464	0.575	0.586	0.621	0.609	0.663	0.607
SA•DMA	N2-H2	0.542	0.503	0.571	0.571	0.577	0.579	0.610
SA•DMA•SUA	N2-H2	0.551	0.548	0.598	0.613	0.583	0.613	0.581
SA•DMA•AM	N1-H1	-	-	-	-	-	-	0.525
	N2-H2	0.489	0.483	0.608	0.553	0.533	0.591	0.567
SA•DMA•AM•SUA	N1-H1	0.420	0.521	0.483	0.321	0.607	0.591	0.677
	N2-H2	0.498	0.411	0.518	0.611	0.501	0.564	0.568

750 Note: N1 is the nitrogen atom on the ammonia (AM) molecule; N2 is the nitrogen atom on the  
 751 dimethylamine (DMA) molecule; H1 is the hydrogen atom on one of the hydroxyl functions of sulfuric  
 752 acid (SA) molecule and bound to N1; H2 is the hydrogen atom on one of the hydroxyl functions of SA  
 753 (SA) molecule and bound to N2.

754

755



756 Table 5. Concentration Ratios between  $SUA \cdot SA \cdot X$  and  $(SA)_2 \cdot X$  Clusters, with  $X = W, AM,$  and  
757 DMA.

SUA/SA	X=(None)	X=W	X=AM	X=DMA
1:1	3.80E+03	5.30E+02	4.11E-03	3.19E-01
10:1	3.80E+04	5.30E+03	4.11E-02	3.19E+00
100:1	3.80E+05	5.30E+04	4.11E-01	3.19E+01
1000:1	3.80E+06	5.30E+05	4.11E+00	3.19E+02
10 000:1	3.80E+07	5.30E+06	4.11E+01	3.19E+03

758